

## A Photoelectron Spectroscopic and Theoretical Study of $B_{16}^-$ and $B_{16}^{2-}$ : An All-Boron Naphthalene

Alina P. Sergeeva,<sup>†</sup> Dmitry Yu. Zubarev,<sup>†</sup> Hua-Jin Zhai,<sup>‡</sup> Alexander I. Boldyrev,<sup>\*,†</sup> and Lai-Sheng Wang<sup>\*,‡</sup>

Department of Chemistry and Biochemistry, Utah State University, 0300 Old Main Hill, Logan, Utah 84322, Department of Physics, Washington State University, 2710 University Drive, Richland, Washington 99354, and Chemical & Materials Sciences Division, Pacific Northwest National Laboratory, MS K8-88, P.O. Box 999, Richland, Washington 99352

Received April 4, 2008; E-mail: boldyrev@cc.usu.edu; ls.wang@pnl.gov

Although boron clusters were experimentally studied shortly after the discovery of the fullerenes,<sup>1</sup> their structural characterization was only possible fairly recently when we combined photoelectron spectroscopy (PES) and theoretical calculations to investigate the structures and bonding of boron clusters.<sup>2–5</sup> Early theoretical studies<sup>6</sup> indicated that small boron clusters do not assume cage-like structures, which are common in bulk boron and compounds; instead, planar or quasi-planar structures were suggested. The combined PES and theoretical studies show indeed boron clusters with up to 15 atoms are planar<sup>2,3,5</sup> and only at  $B_{20}$  does a three-dimensional (3D) structure (double ring) become energetically competitive,<sup>4</sup> whereas  $B_{20}^-$  still remains planar. A recent ion mobility and theoretical study showed that for  $B_n^+$  the double-ring 3D structure becomes competitive at  $B_{16}^+$ .<sup>7</sup>

More interestingly, chemical bonding analyses reveal that  $\pi$  bonding plays an important role in the planar boron clusters.<sup>2,3,5,8</sup> In particular, we have found both aromatic and antiaromatic clusters according to the Hückel rules,<sup>2e,3</sup> analogous to hydrocarbon molecules. In the current work, we focus on  $B_{16}^-$  and  $B_{16}$ , whose structures and bonding have not been characterized. We show that both  $B_{16}^-$  and  $B_{16}$  possess quasi-planar structures ( $C_{2h}$ ). More importantly, we find that addition of an electron to  $B_{16}^-$  results in a perfectly planar ( $D_{2h}$ )  $B_{16}^{2-}$ , which possesses 10  $\pi$  electrons with a  $\pi$  bonding pattern similar to that in naphthalene. Thus,  $B_{16}^{2-}$  can be considered as an “all-boron naphthalene”.

Details of the magnetic-bottle PES apparatus used for this study have been described before.<sup>9</sup> Briefly, the  $B_{16}^-$  cluster was produced by laser vaporization of a  $^{10}B$ -enriched target and was mass-selected using time-of-flight mass spectrometry. PES spectra were obtained at two photon energies, as shown in Figure 1. The resolution of our PES apparatus was  $\Delta E/E \approx 2.5\%$ , that is,  $\sim 25$  meV for 1 eV electrons.

The 266 nm spectrum reveals three broad and well-resolved bands (X, A, B). The broadband widths suggest that there must be significant structural changes between the anion and the neutral final states. The X band defines the ground-state vertical detachment energy (VDE) at  $3.39 \pm 0.04$  eV and an adiabatic detachment energy (ADE) of  $3.25 \pm 0.05$  eV, which also represents the electron affinity of  $B_{16}$ . At 193 nm, the relative intensity of the B band is increased and another broadband C, which overlaps with band B, also becomes prominent. The 193 nm spectrum is less well resolved and beyond 4.8 eV there is a series of overlapping spectral transitions, which are labeled for the sake of discussion. The VDEs of all the spectral features are given in Table 1, compared with theoretical calculations, as discussed in the next section.

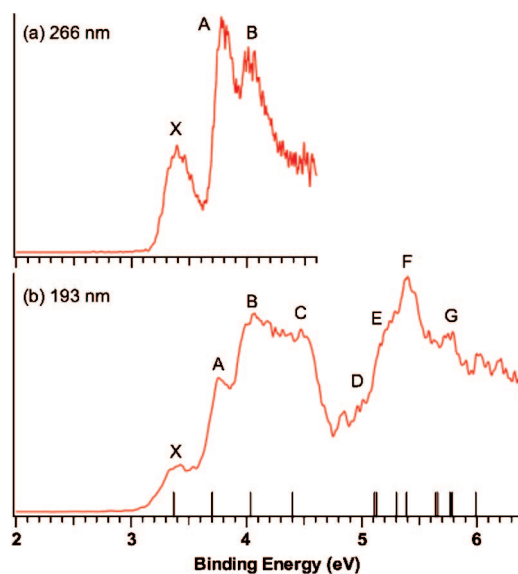


**Figure 1.** Photoelectron spectra of  $B_{16}^-$  at (a) 266 nm (4.661 eV) and (b) 193 nm (6.424 eV). The vertical bars represent the calculated VDEs at the TD-B3LYP level (see Table 1).

Theoretically we first searched for the global minimum of  $B_{16}$  using the gradient embedded genetic algorithm (GEGA) program<sup>10</sup> at the B3LYP/3-21G level of theory and then recalculated geometries of the low-lying isomers at the B3LYP/6-311+G\* level. The lowest energy structures identified for  $B_{16}$  were used as initial structures for  $B_{16}^-$  and  $B_{16}^{2-}$ . The VDEs of  $B_{16}^-$  were calculated using the R(U)CCSD(T)/6-311+G\*, the outer valence green function method [UOVGF/6-311+G(2df)] and the time-dependent density functional theory (DFT) method [TD-B3LYP/6-311+G(2df)] at the B3LYP/6-311+G\* geometries. All calculations were performed using the Gaussian 03 program.<sup>11a</sup> Molecular orbital (MO) visualization was done using the MOLDEN3.4<sup>11b</sup> and MOLEKEL4.3<sup>11c</sup> programs.

The global minimum of  $B_{16}^-$  is shown in Figure 2, **I.1** ( $C_{2h}$ ,  $^2A_u$ ), which is similar to a low-lying isomer found for  $B_{16}^+$ .<sup>7</sup> Alternative structures can be found in Figure S1 in the Supporting Information. The second lowest isomer **I.2** ( $C_s$ ,  $^2A'$ ) is 0.7 kcal/mol (B3LYP/6-311+G\*) and 3.7 kcal/mol (CCSD(T)/6-311+G(2df)//B3LYP/6-311+G\*) higher in energy. The double-ring structure **I.4** of  $B_{16}^-$  ( $C_s$ ,  $^2A'$ ), analogous to the predicted global minimum structure of  $B_{20}$ ,<sup>4</sup> was found to be 36 kcal/mol higher, very different from  $B_{16}^+$ , for which the double-ring structure is a low-lying isomer.<sup>7</sup>

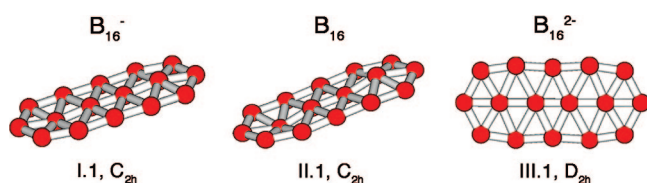
<sup>†</sup> Utah State University.

<sup>‡</sup> Washington State University and Pacific Northwest National Laboratory.

**Table 1.** Comparison of the Experimental Vertical Detachment Energies (VDE) with the Calculated Values of  $B_{16}^-$  (Structure **I.1**). All Energies Are in eV

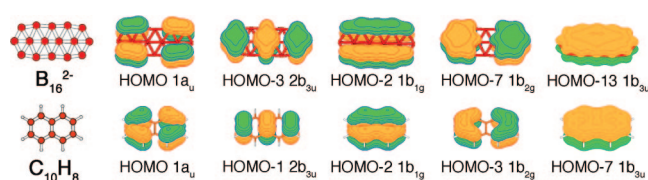
feature	VDE (exptl) <sup>a</sup>	final state and electronic configuration	VDE (theoretical)		
			TD-B3LYP <sup>b</sup>	OVGF <sup>c</sup>	$\Delta$ CCSD(T) <sup>e</sup>
X	3.39 (4)	$^1A_g, 7a_g^2 6b_u^2 4b_g^2 27b_u^2 5b_g^2 5a_u^2 6a_u^0$	3.37	3.57 (0.88)	3.27
A	3.78 (4)	$^3A_g, 7a_g^2 6b_u^2 4b_g^2 27b_u^2 5b_g^2 5a_u^1 6a_u^1$	3.70	3.53 (0.88)	3.76
B	4.03 (4)	$^1A_g, 7a_g^2 6b_u^2 4b_g^2 27b_u^2 5b_g^2 5a_u^1 6a_u^1$	4.03	<i>d</i>	
C	4.4 (1)	$^3B_u, 7a_g^2 6b_u^2 4b_g^2 27b_u^2 5b_g^1 5a_u^2 6a_u^1$	4.40	4.44 (0.88)	
D	~5.0	$^3B_g, 7a_g^2 6b_u^2 4b_g^2 27b_u^2 5b_g^2 5a_u^2 6a_u^1$	5.11	5.36 (0.88)	
		$^1B_u, 7a_g^2 6b_u^2 4b_g^2 27b_u^2 5b_g^1 5a_u^2 6a_u^1$	5.12	<i>d</i>	
E	~5.2	$^3B_u, 7a_g^2 6b_u^2 4b_g^2 27b_u^2 5b_g^2 5a_u^2 6a_u^1$	5.30	5.46 (0.83)	
F	5.40 (10)	$^1B_g, 7a_g^2 6b_u^2 4b_g^2 27b_u^2 5b_g^2 5a_u^2 6a_u^1$	5.39	<i>d</i>	
G	5.6 ~ 6.2	$^3B_g, 7a_g^2 6b_u^1 4b_g^2 27b_u^2 5b_g^2 5a_u^2 6a_u^1$	5.65	5.86 (0.84)	
		$^1B_u, 7a_g^2 6b_u^2 4b_g^2 27b_u^2 5b_g^2 5a_u^2 6a_u^1$	5.66	<i>d</i>	
		$^1B_g, 7a_g^2 6b_u^1 4b_g^2 27b_u^2 5b_g^2 5a_u^2 6a_u^1$	5.77	<i>d</i>	
		$^3A_u, 7a_g^1 6b_u^2 4b_g^2 27b_u^2 5b_g^2 5a_u^2 6a_u^1$	5.78	6.25 (0.83)	
		$^1A_u, 7a_g^1 6b_u^2 4b_g^2 27b_u^2 5b_g^2 5a_u^2 6a_u^1$	5.99	<i>d</i>	

<sup>a</sup> Numbers in parentheses represent the uncertainty in the last digit. <sup>b</sup> VDEs were calculated at TD-B3LYP/6-311+G(2df)/B3LYP/6-311+G\* level of theory. <sup>c</sup> VDEs were calculated at UOVGF/6-311+G(2df)/B3LYP/6-311+G\* level of theory. Values in parentheses represent the pole strength of the OVGF calculation. <sup>d</sup> This transition cannot be calculated at this level of theory. <sup>e</sup> VDEs were calculated at R(U)CCSD(T)/6-311+G\*/B3LYP/6-311+G\* level of theory.

**Figure 2.** The optimized global minimum structures of  $B_{16}^-$  ( $^2A_u$ ),  $B_{16}$  ( $^1A_g$ ), and  $B_{16}^{2-}$  ( $^1A_g$ ) at B3LYP/6-311+G\*.

The VDEs for the global minimum structure **I.1** of  $B_{16}^-$  have been computed using three methods and are compared to the PES data in Table 1. The first two detachment channels are calculated using the  $\Delta$ CCSD(T) method, which yields VDEs in close agreement with the TD-B3LYP method. The OVGF VDEs appear to be off by as much as 0.3 eV compared to the TD-B3LYP values. We have shown previously for smaller  $B_n^-$  ( $n = 10-15$ ) clusters that the TD-B3LYP method gives VDEs in very good agreement with PES data with errors in the range of 0.1–0.2 eV.<sup>3</sup> Indeed, as can be seen from Table 1 and Figure 1b, the VDEs from the first four detachment channels, which are well resolved in the PES spectra, are in excellent agreement with the experiment. The first VDE (X) corresponds to detachment from the singly occupied  $6a_u$ -HOMO with the singlet final state  $^1A_g$ . The second (A) and third (B) VDEs correspond to detachment from the  $5a_u$ -HOMO-1, leading to the triplet ( $^3A_g$ ) and singlet ( $^1A_g$ ) final states, respectively. The fourth VDE (C) derives from detachment from the  $5b_g$ -HOMO-2 leading to the triplet final state ( $^3B_u$ ). The VDE (5.12 eV) for the corresponding singlet state ( $^1B_u$ ) is similar to the next detachment channel from the  $7b_u$ -HOMO-2 with a calculated VDE of 5.11 eV. Higher detachment channels give a series of closely spaced VDEs, consistent with the highly congested PES spectrum in the high binding energy side (Figure 1b). On the other hand, the calculated first VDE (3.69 eV at TD-B3LYP, Table S1) for the second lowest isomer (**I.2** in Figure S1) is significantly higher than the experimental value of 3.39 eV and this isomer can be ruled out as a contributor to the experiment. The good agreement between the calculated and experimental VDEs for structure **I.1** provides considerable credence for its being the global minimum for  $B_{16}^-$ .

Structure **I.1** is quasi-planar because two of the four inner B atoms are slightly out of plane by 0.08 Å. We note that the global minimum of  $B_{16}$  is similar to that of  $B_{16}^-$  but with more severe out-of-plane distortions by 0.24 Å (**II.1** in Figure 2), consistent with the broad ground-state transition in the PES spectrum (Figure

**Figure 3.** Comparison of the structures and  $\pi$  bonding of  $B_{16}^{2-}$  ( $D_{2h}$ ,  $^1A_g$ ) and naphthalene.

1). However, upon addition of an electron to the  $6a_u$ -HOMO of  $B_{16}^-$  ( $C_{2h}$ ,  $^2A_u$ ), we find that the resulting  $B_{16}^{2-}$  dianion becomes a perfect planar ( $D_{2h}$ ) and closed-shell ( $^1A_g$ ) species (**III.1**, Figure 2). More interestingly, further analyses of the canonical MOs of  $B_{16}^{2-}$  show that it possesses 10  $\pi$  electrons and its  $\pi$ -system is analogous to that of the well-known aromatic naphthalene (Figure 3). Thus,  $B_{16}^{2-}$  can be considered as an “all-boron naphthalene”, adding a new member to the hydrocarbon analogues of boron clusters.

It is interesting to note that upon removal of two  $\pi$  electrons from the HOMO of  $B_{16}^{2-}$  the neutral  $B_{16}$  becomes  $\pi$ -antiaromatic and undergoes out-of-plane deformations, analogous to the out-of-plane distortion in the classical antiaromatic cyclooctatetrene ( $C_8H_8$ ). In  $B_{16}$ , two of the four inner boron atoms (at the terminal positions) distort above and below the molecular plane by 0.24 Å (Figure 2), respectively. The open shell  $B_{16}^-$  is in between the  $\pi$ -antiaromatic  $B_{16}$  and the  $\pi$ -aromatic  $B_{16}^{2-}$  and thus suffers much smaller out-of-plane distortions by only 0.08 Å.

The  $\sigma$  bonding patterns in  $B_{16}^{2-}$  are also very interesting and should play important roles in shaping its overall planar structure. It is elucidated using the recently developed adaptive natural density partitioning (AdNDP) method (Zubrev, D. Yu.; Boldyrev, A. I., to be published), which is an extension of the popular natural bond orbital (NBO) analysis. This approach leads to partitioning of the charge density into elements with the highest possible degree of localization of electron pairs. If some part of the density cannot be localized in this manner, it is left “delocalized” (*i.e.*, localized on several atoms in the system), giving rise to  $n$ -center two electron ( $nc-2e$ ) bonds. Thus, AdNDP incorporates naturally the idea of delocalized (globally aromatic) bonds and achieves seamless description of chemical bonding in the most general sense.

According to our AdNDP analysis shown in Figure 4, the  $\sigma$ -bonding framework of  $B_{16}^{2-}$  consists of 12 peripheral  $2c-2e$  B–B bonds with occupation numbers above 1.89 lel, six  $3c-2e$

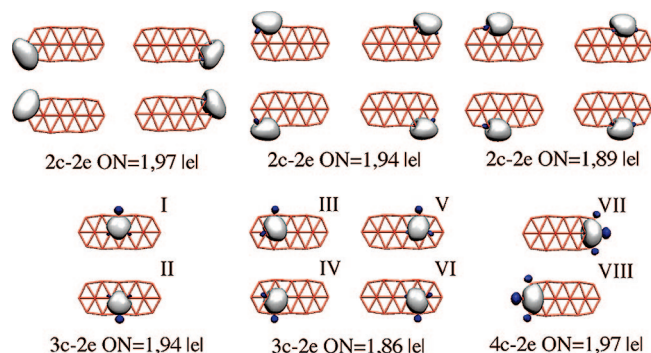


**Figure 4.** Localized nc-2e  $\sigma$ -bonds and occupation numbers in  $B_{16}^{2-}$  obtained by AdNDP analyses.

bonds with occupation number above 1.86 lel, and two 4c-2e bonds with the occupation number 1.97 lel. The four inner boron atoms are bonded to the peripheral boron ring via the 3c-2e and 4c-2e bonds. Out of the twenty canonical valence  $\sigma$ -MOs (Figure S2), twelve ( $3b_{3g}$ ,  $4b_{1u}$ ,  $3b_{1u}$ ,  $2b_{3g}$ ,  $3a_g$ ,  $2b_{2u}$ ,  $2b_{1u}$ ,  $1b_{3g}$ ,  $1b_{2u}$ ,  $2a_g$ ,  $1b_{1u}$ ,  $1a_g$ ) are responsible for the formation of the above-mentioned 2c-2e peripheral B-B bonds formed from the sp-hybridized AOs of boron atoms. The other eight valence canonical  $\sigma$ -MOs ( $5b_{2u}$ ,  $4b_{3g}$ ,  $5b_{1u}$ ,  $6a_g$ ,  $4b_{2u}$ ,  $3b_{2u}$ ,  $5a_g$ ,  $4a_g$ ) form delocalized  $\sigma$ -bonds, formally satisfying the  $4n$  rule for  $\sigma$ -antiaromaticity. This may be responsible for the globally elongated shape of  $B_{16}^{2-}$ , in contrast to the perfectly circular shape of  $B_8^{2-}$  and  $B_9^-$ , which are both  $\pi$ - and  $\sigma$ -aromatic.<sup>2c</sup>

To assess the viability of using  $B_{16}^{2-}$  as building blocks for cluster-assembled nanomaterials, we also optimized structures of  $B_{16}^{2-}$  stabilized by two  $Li^+$  cations in  $Li_2B_{16}$  (Figure S3). We found that the planar  $B_{16}^{2-}$  unit is quite flexible and can be bend or "rippled" upon coordination by  $Li^+$ . This flexibility is probably due to the relatively weak delocalized, in-plane B-B  $\sigma$  bonding, in contrast to the strong C-C  $\sigma$ -bond that forms the framework of naphthalene. Other than the bending distortion induced by  $Li^+$ , the bonding and structural integrity of  $B_{16}^{2-}$  are not altered significantly in  $Li_2B_{16}$ , suggesting its stability and viability as a structural and material building blocks.

Boron clusters with 6  $\pi$ -electrons have been found before, including,  $B_8^{2-}$  and  $B_9^-$ ,<sup>2c</sup>  $B_{10}$ ,  $B_{11}^-$ , and  $B_{12}$ ,<sup>3</sup> as well as  $B_{13}^+$ ,<sup>8</sup> which can be viewed as all-boron analogues of benzene. Globally  $\pi$ -antiaromatic boron clusters with 8  $\pi$ -electrons have also been found, including  $B_{13}^-$  and  $B_{14}$ ,<sup>3</sup> as well as  $B_{16}$ , which can be viewed as analogues of antiaromatic cyclobutadiene or cyclooctatetrene. Here we show that  $B_{16}^{2-}$  with 10  $\pi$ -electrons is an all-boron analogue of naphthalene. A natural question is if we can extend this analogy further to larger all-boron  $\pi$ -aromatic systems and find analogues of anthracene or other polycyclic aromatic hydrocarbons, which are being actively pursued in our laboratories.

**Acknowledgment.** The experimental work done at Washington State University was supported by the National Science Foundation (Grant DMR-0503383) and was performed at the W. R. Wiley Environmental Molecular Sciences Laboratory, a national scientific

user facility sponsored by DOE's Office of Biological and Environmental Research and located at Pacific Northwest National Laboratory, which is operated for DOE by Battelle. The theoretical work done at Utah State University was supported by the National Science Foundation (Grant CHE-07148510).

**Supporting Information Available:** Complete ref 11a, calculated vertical detachment energies for the low-lying  $B_{16}^-$  isomer (structure I.2, Table S1), alternative optimized structures of  $B_{16}^-$ ,  $B_{16}$ , and  $B_{16}^{2-}$  (Figure S1), valence canonical  $\sigma$ -MOs of  $B_{16}^{2-}$  (Figure S2), optimized structures of  $Li_2B_{16}$  (Figure S3), and total energies and Cartesian coordinates for all the optimized structures of  $B_{16}^-$ ,  $B_{16}$ ,  $B_{16}^{2-}$  (Table S2) and  $Li_2B_{16}$  (Table S3). This material is available free of charge via the Internet at <http://pubs.acs.org>.

## References

- (1) (a) Hanley, L.; Anderson, S. L. *J. Phys. Chem.* **1987**, *91*, 5161. (b) Hanley, L.; Anderson, S. L. *J. Chem. Phys.* **1988**, *89*, 2848. (c) Hanley, L.; Whitten, J. L.; Anderson, S. L. *J. Phys. Chem.* **1988**, *92*, 5803. (d) Hintz, P. A.; Ruatta, S. A.; Anderson, S. L. *J. Chem. Phys.* **1990**, *92*, 292. (e) Ruatta, S. A.; Hintz, P. A.; Anderson, S. L. *J. Chem. Phys.* **1991**, *94*, 2833. (f) Hintz, P. A.; Sowa, M. B.; Ruatta, S. A.; Anderson, S. L. *J. Chem. Phys.* **1991**, *94*, 6446. (g) Sowa-Resat, M. B.; Smoloff, J.; Lapiki, A.; Anderson, S. L. *J. Chem. Phys.* **1997**, *106*, 9511. (h) La Placa, S. J.; Roland, P. A.; Wynne, J. J. *Chem. Phys. Lett.* **1992**, *190*, 163.
- (2) (a) Zhai, H. J.; Wang, L. S.; Alexandrova, A. N.; Boldyrev, A. I. *J. Chem. Phys.* **2002**, *117*, 7917. (b) Alexandrova, A. N.; Boldyrev, A. I.; Zhai, H. J.; Wang, L. S.; Steiner, E.; Fowler, P. W. *J. Phys. Chem. A* **2003**, *107*, 1359. (c) Zhai, H. J.; Wang, L. S.; Alexandrova, A. N.; Boldyrev, A. I.; Zakrzewski, V. G. *J. Phys. Chem. A* **2003**, *107*, 9319. (d) Kuznetsov, A. E.; Boldyrev, A. I. *Struct. Chem.* **2002**, *13*, 141. (e) Zhai, H. J.; Alexandrova, A. N.; Birch, K. A.; Boldyrev, A. I.; Wang, L. S. *Angew. Chem., Int. Ed.* **2003**, *42*, 6004. (f) Alexandrova, A. N.; Boldyrev, A. I.; Zhai, H. J.; Wang, L. S. *J. Phys. Chem. A* **2004**, *108*, 3509. (g) Alexandrova, A. N.; Zhai, H. J.; Wang, L. S.; Boldyrev, A. I. *Inorg. Chem.* **2004**, *43*, 3552. (h) Alexandrova, A. N.; Boldyrev, A. I.; Zhai, H. J.; Wang, L. S. *J. Chem. Phys.* **2005**, *122*, 054313. (i) Alexandrova, A. N.; Kayle, E.; Boldyrev, A. I. *J. Mol. Mod.* **2006**, *12*, 569. (j) Zhai, H. J.; Wang, L. S.; Zubarev, D. Y.; Boldyrev, A. I. *J. Phys. Chem. A* **2006**, *110*, 1689.
- (3) Zhai, H. J.; Kiran, B.; Li, J.; Wang, L. S. *Nat. Mater.* **2003**, *2*, 827.
- (4) (a) Kiran, B.; Bulusu, S.; Zhai, H. J.; Yoo, S.; Zeng, X. C.; Wang, L. S. *Proc. Natl. Acad. Sci. U.S.A.* **2005**, *102*, 961. (b) An, W.; Bulusu, S.; Gao, Y.; Zeng, X. C. *J. Chem. Phys.* **2006**, *124*, 154310.
- (5) (a) Alexandrova, A. N.; Boldyrev, A. I.; Zhai, H. J.; Wang, L. S. *Coord. Chem. Rev.* **2006**, *250*, 2811. (b) Zubarev, D. Y.; Boldyrev, A. I. *J. Comput. Chem.* **2007**, *28*, 251.
- (6) (a) Bonacic-Koutecky, V.; Fantucci, P.; Koutecky, J. *Chem. Rev.* **1991**, *91*, 1035. (b) Kawai, R.; Weare, J. H. *J. Chem. Phys.* **1991**, *95*, 1151. (c) Kawai, R.; Weare, J. H. *Chem. Phys. Lett.* **1992**, *191*, 311. (d) Martin, J. M. L.; François, J. P.; Gijbels, R. *Chem. Phys. Lett.* **1992**, *189*, 529. (e) Kato, H.; Yamashita, K.; Morokuma, K. *Chem. Phys. Lett.* **1992**, *190*, 361. (f) Boustani, I. *Int. J. Quantum Chem.* **1994**, *52*, 1081. (g) Boustani, I. *Chem. Phys. Lett.* **1995**, *233*, 273. (h) Boustani, I. *Chem. Phys. Lett.* **1995**, *240*, 135. (i) Ricca, A.; Bauschlicher, C. W., Jr. *Chem. Phys.* **1996**, *208*, 233. (j) Boustani, I. *Surf. Sci.* **1997**, *370*, 355. (k) Boustani, I. *Phys. Rev. B* **1997**, *53*, 16426. (l) Nie, J.; Rao, B. K.; Jena, P. *J. Chem. Phys.* **1997**, *107*, 132. (m) Gu, F. L.; Yang, X.; Tang, A. C.; Jiao, H.; Schleyer, P. v. R. *J. Comput. Chem.* **1998**, *19*, 203. (n) Cao, P. L.; Zhao, W.; Li, B. X.; Song, B.; Zhou, X. Y. *J. Phys.: Condens. Matter* **2001**, *13*, 5065.
- (7) Oger, E.; Crawford, R. M.; Kelting, R.; Weis, P.; Kappes, M. M.; Ahlrichs, R. *Angew. Chem., Int. Ed.* **2007**, *46*, 8503.
- (8) (a) Fowler, J. E.; Ugalde, J. M. *J. Phys. Chem. A* **2000**, *104*, 397. (b) Aihara, J. *J. Phys. Chem. A* **2001**, *105*, 5486. (c) Aihara, J.; Kanno, H.; Ishida, T. *J. Am. Chem. Soc.* **2005**, *127*, 13324.
- (9) Wang, L. S.; Cheng, H. S.; Fan, J. *J. Chem. Phys.* **1995**, *102*, 9480.
- (10) (a) Alexandrova, A. N.; Boldyrev, A. I.; Fu, Y. J.; Wang, X. B.; Wang, L. S. *J. Chem. Phys.* **2004**, *121*, 5709. (b) Alexandrova, A. N.; Boldyrev, A. I. *J. Chem. Theory and Comput.* **2005**, *1*, 566.
- (11) (a) Frisch, M. J.; et al. *Gaussian 03*, revision D.01; Gaussian, Inc.: Wallingford, CT, 2004. (b) Schaftenaar, G. *MOLDEN 3.4*; CAOS/CAMM Center: The Netherlands, 1998. (c) Portmann, S. *MOLEKEL*, version 4.3; CSCS/ETHZ: Zurich, Switzerland, 2002.

JA802494Z